Title

Interstitial Matrix Prevents Therapeutic Ultrasound From Causing Inertial Cavitation in Tumescent Subcutaneous Tissue

Journal

Ultrasound in Medicine & Biology, 44(1)

Authors

Koulakis, John Pandelis
Rouch, Joshua
Huynh, Nhan
et al.

Publication Date

2018

Data Availability

The data associated with this publication are within the manuscript.

Peer reviewed

Interstitial matrix prevents therapeutic ultrasound from causing inertial cavitation in tumescent subcutaneous tissue

John P. Koulakis[a,*], Joshua Rouch[b], Nhan Huynh[b], Genia Dubrovsky[b], James C. Y. Dunn[c], Seth Putterman[a]

[a]*Department of Physics and Astronomy, University of California Los Angeles, Los Angeles, California 90095, USA*

[b]*Department of Surgery, Division of Pediatric Surgery, University of California Los Angeles, Los Angeles, California 90095, USA*

[c]*Department of Surgery. Division of Pediatric Surgery, Stanford Children's Health, 300 Pasteur Drive, Alway M116, Stanford, California 94305, USA*

Abstract

We search for cavitation in tumescent subcutaneous tissue of a live pig under application of pulsed, 1 MHz ultrasound at 8 W cm^{-2} spatial peak, pulse-averaged intensity, and find no evidence of broadband acoustic emission indicative of inertial cavitation. These acoustic parameters are representative of those used in external-ultrasound-assisted-lipoplasty and in physical therapy and our null result brings into question the role of cavitation in those applications. Comparison of broadband acoustic emission from a suspension of ultrasound contrast agent in bulk water to one injected subcutaneously indicates that the interstitial matrix suppresses cavitation, and provides an additional mechanism behind the apparent lack of *in-vivo* cavitation to supplement the "absence of nuclei" explanation offered by the literature. We also find a short-lived cavitation signal in normal, non-tumesced tissue that disappears after the first pulse, consistent with cavitation nuclei depletion *in-vivo*.

Keywords: Cavitation, Tumescent Injection, Ultrasound, Nuclei Depletion, Ultrasound-Assisted Lipoplasty, Therapeutic Ultrasound

Introduction

Ultrasound is a technology with high potential for a wealth of biomedical applications (Goertz and Hynynen, 2016; Mitragotri, 2005). Generally operating at intensities of ∼1-10 W cm^{-2}, "therapeutic" ultrasound has been evaluated for applications such as thrombolysis (Datta et al., 2006; Braaten et al., 1997), sonophoresis (Polat et al., 2010), sonoporation (Tomizawa et al., 2013), lipoplasty (Cook Jr., 1997), and accelerated wound healing (Hart, 1998; Cullum et al., 2010). At much higher intensities, >1000 W cm^{-2}, High-Intensity-Focus-Ultrasound (HIFU) (Kennedy et al., 2003) is used as a non-invasive means of lithotripsy, histotripsy, and tissue ablation.

*Corresponding Author: John Koulakis, Email: koulakis@physics.ucla.edu.

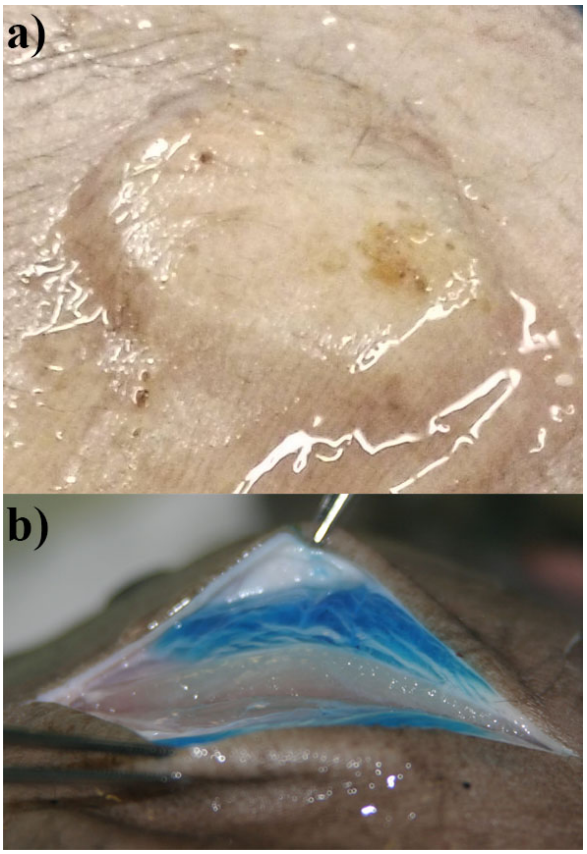

Figure 1: a) Weal left by 10 mL bolus tumescent injection into the subcutaneous tissue of a pig is about 4 cm in diameter. b) Slicing into a tumescent injection of blue-dyed saline and pulling the skin apart reveals that the liquid is trapped within the subcutaneous tissue. The blue region is about 1 cm thick. Notice that the liquid does not run from the tumescent tissue, but is instead held in place.

Whether ultrasound is considered safe for diagnostic purposes, and whether it is effective for other applications, depends critically on whether cavitation occurs *in-vivo* (Holland et al., 1996). There is no doubt that cavitation exists at the high intensities of focused ultrasound, and that it could exist - if proper cavitation nuclei are present - at much lower intensities (Holland and Apfel, 1989; Holland et al., 1992). This article focuses on intensities in the 1-10 W cm^{-2} therapeutic regime that are strong enough to cause cavitation in bulk liquid, but do not reliably cause cavitation in tissue. The apparent lack of cavitation nuclei *in-vivo* has the dual effect of making diagnostic ultrasound safe at higher intensities (Church, 2002), but also hinders the use of cavitation for therapeutic applications. Controlling the location of cavitation inception, growth, and sustentation is a problem that has been mostly solved at high intensities (Hockham et al., 2010; Xu et al., 2004), but its difficulty at lower intensities has slowed the adoption of therapeutic ultrasound technology. The development of ultrasound contrast agents (Keller et al., 1989) and phase-shift nanodroplets (Rapoport, 2012) has provided a convenient method of introducing cavitation nuclei into the body to address the inception problem.

Cavitation, for our purposes, is defined as the expansion, compression, and dynamics of gas pockets in liquid or tissue in response to sound pressure oscillations. It can be "stable," characterized by relatively small amplitude oscillations that result in an emission spectrum of harmonics and half-odd-integer harmonics (Lauterborn, 1976) (ultra-harmonics), or "inertial," characterized by high-amplitude, chaotic oscillations resulting in violent collapse and broadband sound emission (Frohly et al., 2000; Hauptmann et al., 2012). A specified ultrasound frequency will resonantly excite optimally sized bubbles (Minnaert, 1933; Leighton, 1994) (3.7 μm radius at 1 MHz in water), minimizing the cavitation threshold for that pair, while the ultrasound intensity determines the range of bubble size that can be driven to cavitate (Holland and Apfel, 1989). Therefore, whether or not ultrasound of a given frequency and intensity induces cavitation is determined by the size distribution of gas pockets (cavitation nu-

clei) present in the medium.

Time-averaged (over the sound period) bubble dynamics in sonicated free-liquid can be very rich (Neppiras and Coakley, 1976; Plesset and Prosperetti, 1977; Lauterborn and Kurz, 2010), displaying phenomena such as streaking (translational motion), rectified-diffusion (Hsieh and Plesset, 1961; Louisnard and Gomez, 2003), coalescence (Crum, 1975), and fission from surface mode instabilities (Fransecutto and Nabergoj, 1978) or asymmetric collapse (Brennen, 2002). In particular, rectified-diffusion is the process whereby an oscillating bubble will grow because more gas diffuses inwards during the bubble's expansion than diffuses outwards during the compression thanks to the difference in the bubble's surface area. This process has been the basis for some to argue (ter Haar et al., 1982; Crum and Hansen, 1982) that low levels of ultrasound induce bubble growth in tissue. Others have pointed out that there is little range in the relevant parameter space for rectified diffusion to occur without almost immediate inertial cavitation (Church, 1988).

Decades of searching for cavitation *in-vivo* (Holland et al., 1996; Frizzell et al., 1983; Haar et al., 1982) have found that, aside from sensitive areas of the body such as the lungs and intestines, cavitation exists, but only at very high amplitudes that far surpass those required in free liquid. Nightingale et al. (2015) reviews studies with positive cavitation results, and puts the threshold for cavitation at 1 MHz to be greater than 5 MPa peak rarefactional pressure. It is not a robust, reliably-occurring phenomenon at typical diagnostic or therapeutic levels. One hypothesis to explain this is that the body is completely free of cavitation nuclei, but the phenomenon of decompression sickness ("the bends") provides a counter example (Tikuisis, 1986; Papadopoulou et al., 2013; Blatteau et al., 2006). A more refined hypothesis is that there are no cavitation nuclei of the appropriate size.

Routinely used in tumescent anesthesia and liposuction (Klein, 1987), tumescent injections infuse large volumes of physiological saline into adipose and subcutaneous tissue, causing it to expand and become firm. Anesthetics, vasoconstrictors (Klein, 1990), antibiotics (Silberg, 2013; Klein, 2014), or other additives are routinely mixed into the tumescent solution for specific effects. The tumescent technique eliminates the need for systemic anesthesia, reduces overall blood loss, and shortens recovery time (Klein, 1993). Ultrasound is often applied either internally (Zocchi, 1992) or externally (Cook Jr., 1997; D'Andrea et al., 2008; Silberg, 1998; Rosenberg and Cabrera, 2000; Mendes, 2000), and is hypothesized to exert fat loosening or emulsifying effects through cavitation or other means (Coleman et al., 2009; Gasperoni and Salgarello, 2000; Rohrich et al., 2000). Internal Ultrasound-Assisted Lipoplasty (IUAL) employs probes that vibrate underneath the skin at $\sim$ 35 kHz to mechanically disrupt adipose tissue, whereas External Ultrasound-Assisted Lipoplasty (EUAL) attempts to create similar acoustic conditions with a $\sim$ 1 MHz transducer applied on the skin surface. Both methods have been demonstrated to cause cavitation in bulk water (Weninger et al., 1999, 2000), but the existence of cavitation in tumescent tissue has not been verified in either case. As the ultrasound intensities of EUAL ($2-3$ W cm^{-2}) are $\sim 100\times$ lower than cavitation thresholds of non-tumesced tissue (Nightingale et al., 2015; Center for Devices and Radiological Health, 2008), the role of

cavitation in EUAL is in question.

In this paper, we investigate whether a tumescent injection of physiological (0.9%) saline (Figure 1) can provide sufficient nuclei to seed inertial cavitation *in-vivo* and thereby lower cavitation thresholds to EUAL levels. Besides providing nuclei, the expansion of tissue under tumesced conditions might lower the cavitation threshold in and of itself, thanks to the much larger water fraction. Indeed, a close inspection of figure 1b suggests a $3-4\times$ volumetric expansion ratio, saline fraction of 65-75%, and a cavitation threshold much closer to that in bulk fluid. After tumescent injection into healthy, live pigs, we search for inertial cavitation by applying therapeutic ultrasound and listening for broadband acoustic scattering that is indicative of the chaotic motion of bubbles undergoing inertial cavitation (Frohly et al., 2000; Hauptmann et al., 2012). Injections of ultrasound contrast agent provide a positive control. We also test a freshly prepared suspension of powdered cefazolin, an antibiotic routinely added to tumescent solutions (Silberg, 2013), to see whether motes in the powder provide a source of nuclei.

Materials and Methods

Figure 2 is a block diagram of the cavitation excitation and detection system. The drive signal is made by chopping a continuous-wave signal (output of DS345 function generator, Stanford Research Systems, Sunnyvale, CA, USA) with the help of a Stanford Research Systems DG535 pulse generator and high-isolation TTL switch (MiniCircuits ZASWA-2-50DR+, Brooklyn, NY, USA). It is amplified with an ENI A150 high-power amplifier (Rochester, NY, USA) and taken to the transducer. A custom-designed transducer and passive cavitation detector (PCD) combination ultrasound head (Precision Acoustics, Dorchester, UK), seen in figure 3a, conveniently allows simultaneous drive and pick-up of acoustic scattering. The axial transducer is a flat single crystal and is 23 mm in diameter. It generates a beam of 20 mm - 6 dB diameter at a distance of 17 mm from the aperture. Beam transverse and axial profiles (figures 3b and 3c) were obtained with a Precision Acoustics 1 mm needle hydrophone (with packaged preamplifier and DC coupler) in a degassed water tank. The hydrophone was calibrated by the manufacturer to an accuracy of 20%. We drive the transducer at a frequency of 987 210 Hz, arbitrarily chosen near the peak of its response curve, but will refer to it simply as 1 MHz below.

For comparison, the beam profile of a Mettler ME8010 ultrasound handle (flat, single crystal, 44 mm diameter active area, Mettler Electronics Corp., Anaheim, USA) driven by a Mettler ME800 Silberg T.P.S. Tissue Preparation System commonly used in EUAL is also included in figure 3. This particular EUAL system is the strongest used in the industry. Although its maximum setting is nominally 3 W cm^{-2}, our measurements in a degassed water tank show a peak intensity of 8 W cm^{-2} on axis. We therefore use 8 W cm^{-2} in our cavitation search.

The PCD of our custom ultrasound head is a film of PVDF whose surface is in the shape of an annular cone. It is designed to be sensitive to a cigar-shaped region collinear with the axis, about 3 mm in diameter, between 8 to 30 mm in front of the transducer's aperture. Although the ultrasonic beam width is much larger than the 3 mm diameter sensitivity zone of the

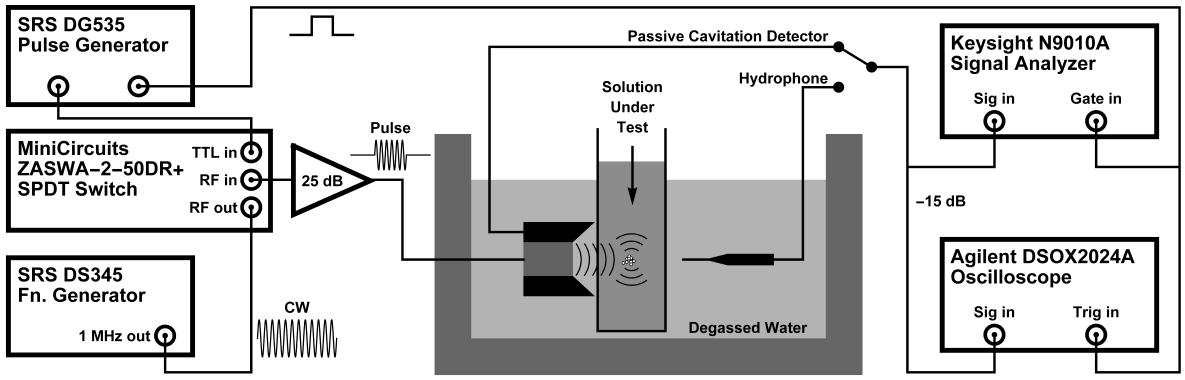

Figure 2: Block diagram of the drive and signal acquisition system. 1 MHz pulses are generated by chopping a continuous wave signal with a TTL-driven switch. Our transducer/PCD combo handle (Figure 3) is either placed in a degassed water tank for calibration (pictured) or held against a pig for the experiment (not shown). A time trace of the broadband acoustic noise level in a 51 kHz bandwidth centered at 1.75 MHz is obtained with a gated signal analyzer operating in zero-span mode.

PDC, the highest ultrasound intensities are on axis where the PCD is most sensitive (see figure 3b). The empty space internal to the conical PCD surface was filled with 2% agarose gel to facilitate acoustic coupling to pigs, and was left in place during calibration. A -15 dB splitter takes a small part of the PCD signal to an Agilent DSOX2024A oscilloscope (Santa Clara, CA, USA) for time-domain viewing. The main portion of the signal goes to a Keysight N9010A signal analyzer (Santa Rosa, CA, USA).

Our detection system is calibrated with size isolated microbubbles (SIMB1-2, lipid-coated fluorocarbon bubbles 1.7 ± 0.6 μm mean diameter $\pm$ standard deviation, Advanced Microbubbles Laboratories, Boulder, USA) in a degassed water tank. A thin plastic bag (Nasco Whirl-Pak, Fort Atkinson, WI, USA) was filled with a suspension of microbubbles and placed in front of the combination ultrasound head as shown in figure 2. The liquid level in the bag was kept slightly above that of the surrounding degassed water to keep the bag taught. 1 MHz ultrasound pulses of 200 ms length, 3 W cm^{-2}, were applied. This intensity was sufficient to pop the microbubbles, so we included a slowly rotating magnetic stirrer to keep the suspension well-mixed. The pulse frequency was slow enough (0.7 Hz) to avoid local bubble depletion effects, which were observed for pulse rates greater than 2 Hz. Global bubble depletion was not a concern because of the large bag volume. We repeated this experiment with tap water and physiological saline separately instead of the microbubble suspension to qualitatively compare the dynamics of the cavitation signal from different fluids.

The power spectra of the PCD signal shown in figure 4a are instructive for understanding our signal acquisition scheme. The spectra are averages of 10 traces acquired with a 51 kHz resolution bandwidth between 150-175 ms after the pulse begins, when the signal has stabilized. We ignore the drive harmonics because they can be generated by sources other than cavitation, such as the non-linearity of the water or tissue (Blackstock et al., 2008). The ultra-harmonics and broadband (white) acoustic

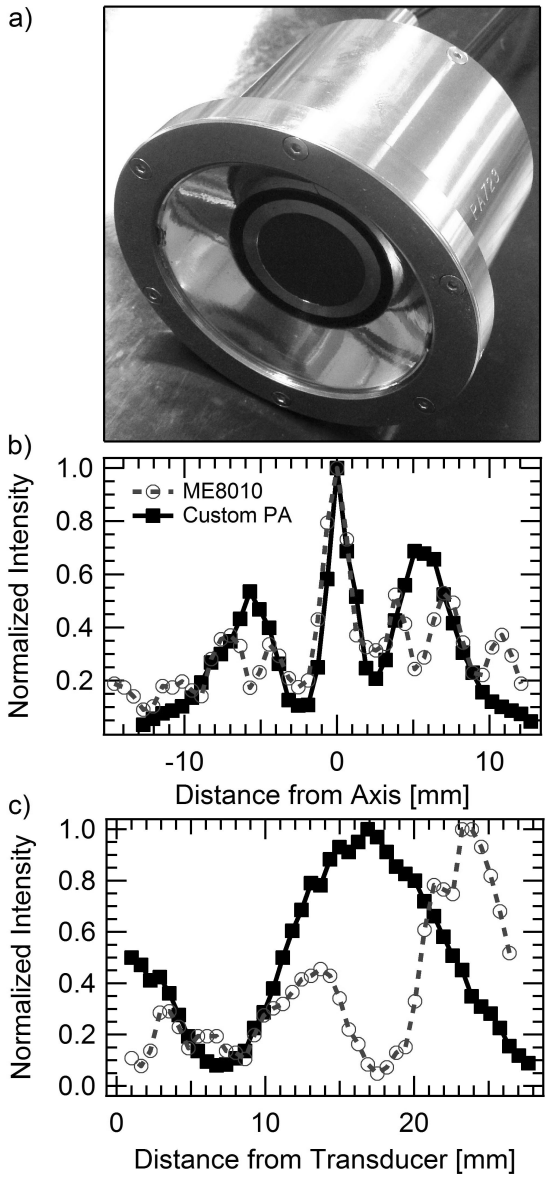

Figure 3: (a) Custom built ultrasound head with axial transducer and annular passive cavitation detector (PCD). Transverse (b) and axial (c) beam profiles generated by our ultrasound head as compared to those generated by a Mettler ME8010 handle driven by a Silberg TPS.

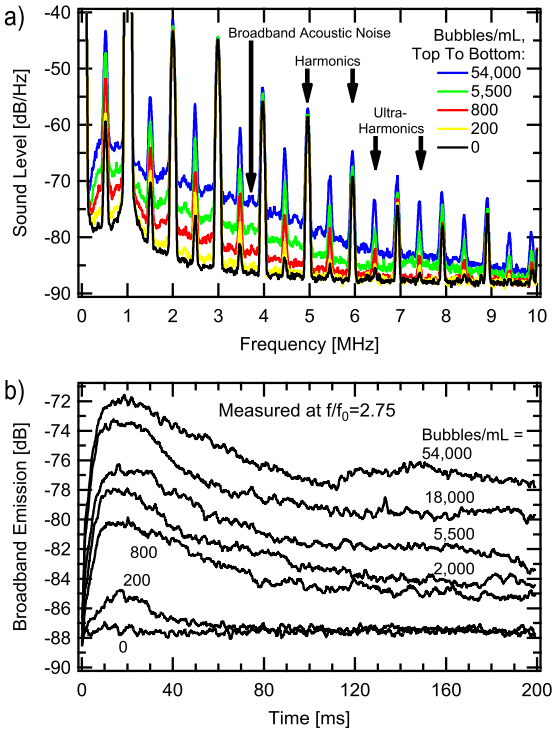

Figure 4: Cavitation of size-isolated microbubbles in a degassed tank provides a calibration of our detection system. The acoustic spectra in (a) show the increase in ultra-harmonic, and broadband noise levels as the microbubble concentration is increased. Setting the signal analyzer to measure the noise power in a small bandwidth at 2.75 MHz over time (zero-span mode) yields the curves in (b). The broadband noise level varies during the ultrasound pulse and stabilizes after about 120 ms. The spectra in (a) were measured after stabilization, between 150-175 ms after the start of the pulse.

noise level are considered better indicators of cavitation in a tank (Lauterborn, 1976; Frohly et al., 2000; Hauptmann et al., 2012). In our experiment, however, we found that the ultra-harmonics were unreliable indicators of cavitation as well. When holding our ultrasound head in contact with dead pigs during preliminary testing, the ultra-harmonic amplitude would undergo large, reproducible changes in response to tilting or adjusting pressure on the ultrasound head. The extreme sensitivity to difficult-to-control variables made working with the ultra-harmonic signal too impractical. We use instead the broadband acoustic noise level as a more reliable cavitation indica-

tor. The broadband noise level for the 0 microbubble mL^{-1} (black) curve in figure 4 is the electronic noise level of our signal analyzer, not acoustic noise. At a concentration of 200 microbubble mL^{-1}, the acoustic noise surpasses the electronic noise. Concentrations as low as 6 mL^{-1} could be detected in the ultra-harmonic signal in the well-controlled environment of a water tank.

Cavitation signals can vary on timescales that are faster than the acquisition time of an entire spectrum, so to capture the full signal dynamics we are forced to measure in a different manner. We set the signal analyzer to operate in zero-span mode, where it records the acoustic power in a given bandwidth over time. Setting it to a frequency where only broadband acoustic noise exists gives the curves in figure 4b, which are averages of 10 measurements at each microbubble concentration. These curves are a measurement of inertial cavitation activity over time, and are the nature of the data we seek to collect from pig tissue.

Measurements were made on the abdomen of a 105 lb, shaved, anesthetized, one-year-old Yucatán pig. The use of all animals in this study was approved by the UCLA Animal Research Committee. Five spots on the abdomen were used to measure the tissue response without an injection, four spots with a 10 mL physiological saline injection, and three spots with a 10 mL, 10 mg mL^{-1} cefazolin injection. An additional six spots were used to inject 10 mL of saline with different concentrations of microbubble ultrasound contrast as a positive control and *in-vivo* sensitivity test for our detection system. We use the term "tumescent fluid" to refer to any of these solutions/suspensions as determined by context. In all cases, the saline was mixed vigorously with air and left to sit to ensure it was in gaseous equilibrium with atmosphere.

The acoustics protocol was to administer five 100 ms long pulses of 1 MHz, 8 W cm^{-2} peak spatial intensity ultrasound at a repetition rate of 1 Hz, and to capture the broadband acoustic noise level at 1.75 MHz during each pulse. We found in preliminary measurements that a cavitation signal existed only during the first pulse (described below) and that continued pulsing (or continuous wave application) produced no further signal. Injections with high microbubble concentrations were an exception to this, and did show some signal on the second pulse, albeit dramatically reduced. There was no signal on any third pulse.

Ultrasound gel needs to be applied between the transducer and the pig to prevent acoustic mismatch. We found, however, that microbubbles within this gel layer can generate a cavitation signal, and so one has to degas the gel before the experiment can be done. Unfortunately, if one puts the usual ultrasound gel under a vacuum, it froths up and can be pulled into the vacuum pump. Instead, we used a less viscous gel marketed at our local pharmacy as "silkie smooth" personal lubricant that allowed bubbles to rise faster, and we were able to degas without problems. We verified that there was no cavitation signal coming from the gel by applying it to an ultrasound-absorbing sheet (Precision Acoustics Aptflex F28, >22dB echo reduction) and performing the measurement protocol before and after the experiment. The curve labeled "background" in subsequent plots is the average signal acquired with this procedure.

Since the cavitation threshold in tissue is generally considered far higher than the 8 W cm^{-2} we use, the locations without an injection were intended to be negative con-

trols. There was, however, a signal that existed only during the first pulse, as will be discussed below. This tissue-only first-pulse signal would obscure interpretation of a cavitation signal coming from tumesced tissue, so the protocol was modified as follows. The injection needle was inserted subcutaneously at the location of planned tumescence, but the liquid was not injected. Gel and the ultrasound head were placed on the pig's skin centered above the needle, and 5 pulses of ultrasound were applied. Then the tumescent solution was injected through the needle while holding the ultrasound head in place, and the measurement was subsequently performed. In this way we are assured that any resulting signal is due to the tumescent injection.

The *in-vivo* sensitivity test for our detection system was done with the first-pulse-suppressing protocol. We injected 10 mL of saline containing various concentrations (10 - 10^6 mL^{-1} in factors of 10) of the same 1-2 μm diameter size isolated microbubbles described above. Ultrasound pulses were applied with the same parameters as above and the PCD signal was recorded.

Results and Discussion

Figure 5 shows the results of the *in-vivo* PCD sensitivity test. Broadband acoustic emission is detectable from solutions with microbubble concentrations fewer than 1000 mL^{-1} and higher, generally consistent with our results in a tank. The first pulse has the largest signal, and each subsequent pulse (not shown) was reduced relative to the previous. Concentrations of 10 (not shown) and 100 mL^{-1} were indistinguishable from the electrical background.

Applying ultrasound to the pig abdomen without tumescence results in the broadband acoustic emission curves in figure 6. A cavitation signal is present for 1 ms during the first pulse only. All subsequent pulses are indistinguishable from background. We interpret this short-lived signal as cavitation nuclei depletion similar to that observed by others in agar phantoms (Hockham et al., 2010). Appropriate cavitation nuclei exist before the first sound pulse, and are quickly depleted upon application of ultrasound. The nucleus population does not have time to recover before the subsequent pulse. The signal amplitude is comparable to that generated by the ultrasound contrast at a concentration of $10^3 - 10^4$ mL^{-1}. Cavitation from crevices on the rough pig skin underneath the gel is a consistent explanation that we cannot rule out. Another intriguing possibility is that the cavitation nuclei are truly inside the body. Previous searches for cavitation *in-vivo* used different ultrasound parameters and detection schemes and may have missed such a short-lived signal. If verified, this would be evidence for cavitation at $\sim 100\times$ lower inten-

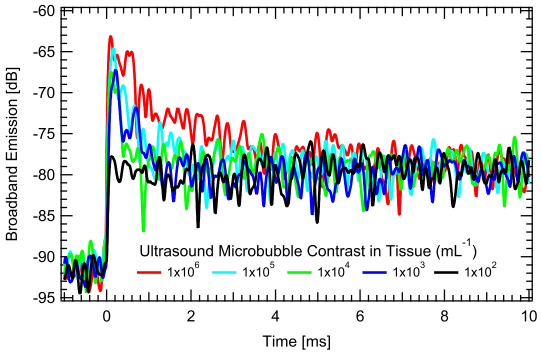

Figure 5: Broadband acoustic emission level from tissue tumesced with 10 mL saline containing various concentrations of 1-2 μm diameter size-isolated microbubbles. The signal at a concentration of 100 mL^{-1} is indistinguishable from electrical background. Pulses after the first (not-shown) have a reduced signal.

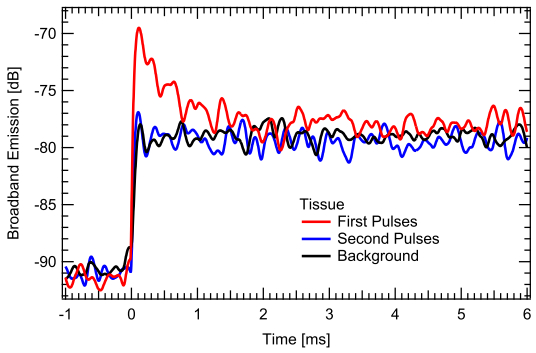

Figure 6: Average broadband acoustic emission level from tissue (no tumescence). A cavitation signal is visible for 1 ms in the first pulse but does not repeat during the second pulse. This behavior is characteristic of cavitation nuclei depletion.

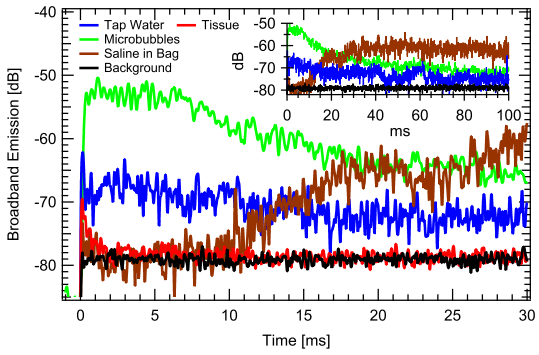

Figure 7: Broadband acoustic emission level from cavitation in different solutions, with inset displaying the signals over a longer time scale. The microbubble curve was measured at a bubble concentration of 42×10^3 mL^{-1}.

sity than accepted thresholds (Nightingale et al., 2015).

None of the 7 tumescent measurements without microbubbles (4 with physiological saline and 3 with 10 mg mL^{-1} cefazolin) resulted in any signal above background and are therefore not presented. The tumescent fluid did not provide a detectable level of fresh cavitation nuclei.

Figure 7 shows the PCD signal from cavitation in fresh tap water, a sealed IV bag of physiological saline, and a microbubble suspension in a tank, to be compared to the signal from tissue taken under the same acoustic parameters. Tap water is assumed to be super-saturated with gas since bubbles on the container wall spontaneously grow when it is left to sit, and visible cavitation clouds readily form in it at low ultrasounds intensities. The cavitation signal turns on immediately, stays relatively flat for the entire pulse duration, and repeats itself on subsequent pulses. Although the precise shape of the curve is not reproducible, the qualitative features we point out are reproducible. The saline bag is assumed to be in gaseous equilibrium because the saline has been in contact with the air inside the bag for years. It was shaken by hand five minutes prior to the measurement and then left to sit. The cavitation signal takes 10 ms to surpass the background level and saturates after 30 ms. Subsequent pulses start at a level above background and reach saturation faster. Without shaking the bag, there is no cavitation signal at these amplitudes. Once again, although the time the cavitation signal surpasses the background level, or saturates, depends on the time since shaking the bag (and how the bag was shaken), the qualitative features we point out are reproducible. We understand this complex behavior as that reported by Hauptmann et al. (2013), where initially small bubbles grow due to rectified diffusion and/or coalescence until they break-up from surface instabilities, eventually reaching a steady state bubble size distribution. As described by Hauptmann et al. (2013), during the pulse off-time, bubbles shrink from dissolution, but may not have enough time to dissolve completely. Emission from the microbubble suspension, on the other hand, starts high, and continues to drop. The ultrasound pops the lipid-coated bubbles and

the fluorocarbon gas dissolves away rapidly because the concentration in the water is zero (Frinking et al., 1999).

The relatively long-lasting cavitation signal from the microbubble suspension in a tank (green curve of figure 7) compared to that from a tumescent injection of a similar suspension (red curve of figure 7) suggests different bubble dynamics inside tumesced tissue and in free-liquid. Physiology textbooks describe the fluid in edematous interstitial tissue as being largely contained in "small pockets and rivulets" within which it is freely flowing (Guyton and Hall, 2006). Based on this, one might expect similar acoustic emission from the tumescent tissue as from the tank - but this is not the case. Figure 1b is a photograph of the cross section of a tumescent injection of blue-dyed saline into the subcutaneous tissue of a dead pig. The total absence of liquid running down the cross section is a dramatic demonstration that the liquid is locked in place within the polymer matrix; it is not free, despite the tissue expanding over four times in thickness. Such a viscoelastic, fibrous, mesh-like environment would presumably favor asymmetric bubble collapse, hinder bubble coalescence, and lead to weaker broadband emission (Yang and Church, 2005; Fogler and Goddard, 1970). It appears that a hydrogel model is more appropriate for tumescent tissue than the rivulet description in textbooks, however we are not aware of any synthetic hydrogel that can withstand a $\sim 4\times$ volume expansion upon injection of fluid without fracturing.

Bubble nuclei must exist in the body to explain phenomena such as decompression sickness in divers. While their size, location within tissue, and generation mechanism is mostly unknown (Blatteau et al., 2006), it is safe to say that they are smaller than a micron in radius. In free-liquid, one might expect them to grow from rectified diffusion upon application of sufficiently high amplitude ultrasound (but see Church (1988) for caveats). If the same were true in tissue, we would expect the cavitation signal to increase initially, as the bubble size grows closer to resonant at 1 MHz (3.7 μm radius) and the oscillation amplitude increases. However, the opposite behavior is observed; the signal decays immediately upon application of ultrasound. Our tentative interpretation is that the nuclei are shrinking, and we propose that negative rectified diffusion may be the cause. For instance, a bubble embedded in tissue would feel little resistance to collapse during the high-pressure part of the sound cycle. There might, however, be a large resistance to expansion because the polymer constituents of tissue are placed under tension (a string yields under compression but is strong in tension). Reminiscent of the "compression-only" oscillation dynamics observed in coated bubbles (de Jong et al., 2007; Marmottant et al., 2005), the result is that the bubble compression is much greater than its expansion, and the mechanism of rectified-diffusion pushes it towards dissolution rather than growth. Fracturing of the original microbubble is another plausible mechanism of nuclei depletion if a mechanism exists to prevent the daughter bubbles from coalescing.

Summary and Conclusion

We studied cavitation in tumescent pig tissue by looking at scattered broadband acoustic noise levels during ultrasound pulses. Our ultrasound intensity of 8 W cm^{-2} was chosen to be representative

of the largest intensities used in therapeutic ultrasound, and particularly external-ultrasound-assisted lipoplasty. This intensity is large enough to cause cavitation in bulk water, but is well below cavitation thresholds in non-tumesced tissue. We expected that the $3-4\times$ tumescent expansion of subcutaneous tissue would lower its cavitation threshold to levels closer to those in bulk fluid, but found a null result. No signal was observed for injections of saline, or an antibiotic solution. One limitation of this work is that our PCD was insensitive to cavitation from bubble concentrations 100 mL^{-1} and fewer, and so we cannot rule out lower levels of cavitation activity.

We did find signals lasting 1-2 ms during the first pulse only, both without an injection, or with an injection of ultrasonic contrast agent, that are consistent with cavitation nuclei depletion *in-vivo*. In the former case, the signal may be due to gas in crevices on the pig's skin. If follow-up studies can verify that it is coming from within the tissue itself, this would be an example of cavitation at $\sim 100\times$ lower intensity than accepted thresholds and would lend credence to cavitation as a mechanism of action of therapeutic ultrasound.

Our results are in line with the growing literature touting the body's suppression of cavitation. The stark contrast between the signals from a microbubble suspension in a tank and one in tumesced tissue suggests that the suppression mechanism is more than simply an absence of adequate nuclei; the tissue microenvironment plays a key role. Tumescent injections do not lower the cavitation threshold to therapeutic ultrasound levels, and even if adequate nuclei are brought in with the fluid, their cavitation is not sustained. Therefore, if externally applied ultrasound at 1 MHz has any effect in lipoplasty, it is not due to sustained cavitation at levels we can detect. We interpret the absence of cavitation as indicating that tumescent injections do not create "small pockets and rivulets" in healthy tissue. However, this study does not rule out the possibility that tissue which is inflamed due to some pathology could cavitate when infused with additional fluid. The infrastructure of pathological tissue might not exhibit the same degree of plasticity and dilation symmetry as that of healthy tissue. Other processes whereby ultrasound in the range of 1-10 W cm^{-2} might interact with tissue include micro-streaming, which is not ruled out by this set of experiments.

Finally we note that this set of experiments was performed on a single pig, and the results cannot be considered complete in the sense that we have not measured the effects of biological variability. Our procedure, however, was refined during a series of preliminary measurements on at least a dozen pigs, whose results are consistent with those we present here. When considering the implications of this study to clinical practice, the systematic variation between pig and human tissue is more of a concern then the variation between pigs, and we propose that measurements on humans would be more interesting than additional pig study.

Acknowledgments

We gratefully acknowledge support from the Paul S. Veneklasen Research Foundation. We thank Barry Silberg and Craig Heller for helpful discussions; Adam Collins, Seth Pree, Alexandra Latshaw, Elvin Chiang, and the UCLA DLAM staff for assistance; and Shylo Stiteler for constructing our vacuum-compatible water tank.

Appendix

Because we record low-level broadband emission synchronously with the high-power sound pulse, there is considerable electrical and acoustic crosstalk between the PCD and the transducer. Fortunately, the sharp filters of the signal analyzer are able to filter out the relatively large drive signal and its harmonics when the center frequency is set between them. But the sound pulse can still be seen in the zero-span signal analyzer output as a high-amplitude spike when the pulse turns on, followed by an increased background level that remains flat during the entire pulse (figure 8, "raw background curve"). To smooth out the broadband acoustic noise trace in post-processing, it is first converted to linear scale (the signal analyzer records in logarithmic scale), then a 5 kHz, 4-pole, digital low-pass filter is applied, followed by conversion back to logarithmic scale. This lowers the fluctuations of the signal from $\sim \pm 10$ dB to $\sim \pm 4$ dB. However, when the high-amplitude spike artifact (~ 80 μs wide) at the pulse turn-on is filtered, it generates an apparent decay visible for 1 ms (figure 8, "filtered without spike blocked"), that masks short-lived, smaller-amplitude signals. To avoid this problem, we cut off the spike by replacing the data values during 100 μs centered on the spike with the value of the data point at the beginning of this interval, and then filtering (figure 8, "filtered with spike blocked"). All data were processed with this protocol.

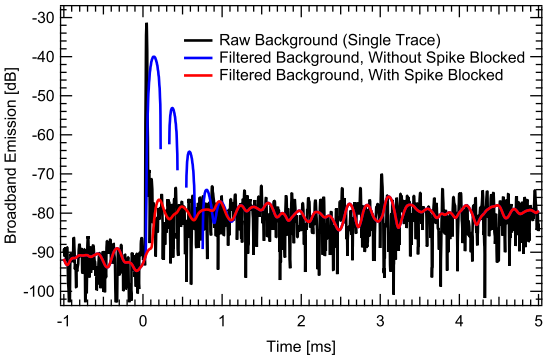

Figure 8: The raw and processed PCD signal acquired when the handle is applied to an ultrasound-absorbing sheet. The trace is post-processed to smooth out noise by chopping the high-amplitude spike at the beginning of the pulse (t=0) and then low-pass filtering with a 5 kHz, 4-pole digital filter.

References

Blackstock DT, Hamilton MF, Pierce AD. Progressive waves in lossless and lossy fluids. In: Nonlinear Acoustics. Acoustical Society of America, Melville, New York, Ch. 4, 2008.

Blatteau JE, Souraud JB, Gempp E, Boussuges A. Gas nuclei, their origin, and their role in bubble formation. Aviation, Space, and Environmental Medicine, 2006;77:1068–1076.

Braaten JV, Goss RA, Francis CW. Ultrasound reversibly disaggregates fibrin fibers. Thrombosis and Haemostasis, 1997;78:1063–1068.

Brennen CE. Fission of collapsing cavitation bubbles. Journal of Fluid Mechanics, 2002;472:153–166.

Center for Devices and Radiological Health. Guidance for industry and FDA staff, information for manufacturers seeking marketing clearance of diagnostic ultrasound systems and transducers. Tech. rep., United States Department of Health and Human Services Food and Drug Administration, 2008.

Church CC. Prediction of rectified diffusion during nonlinear bubble pulsations at biomedical frequencies, 1988;83:2210–2217.

Church CC. Spontaneous homogeneous nucleation, inertial cavitation and the safety of diagnostic ultrasound. Ultrasound in Medicine & Biology, 2002;28:1349–1364.

Coleman KM, 3rd Coleman WP, Benchetrit A. Non-invasive, external ultrasonic lipolysis. Sem-

inars in Cutaneous Medicine and Surgery, 2009;28:263–7.

Cook Jr. WR. Utilizing external ultrasonic energy to improve the results of tumescent liposculpture. Dermatologic Surgery, 1997;23:1207–1211.

Crum LA. Bjerknes forces on bubbles in a stationary sound field. The Journal of the Acoustical Society of America, 1975;57:1363–1370.

Crum LA, Hansen GM. Growth of air bubbles in tissue by rectified diffusion. Physics in Medicine and Biology, 1982;27:413.

Cullum N, Al-Kurdi D, Bell-Syer SE. Therapeutic ultrasound for venous leg ulcers. Cochrane Database of Systematic Reviews, 2010.

D'Andrea F, Ferraro GA, Nicoletti GF, Francesco FD. External ultrasound-assisted lipectomy: Effects on abdominal adipose tissue. Plastic and Reconstructive Surgery, 2008;121:355e–356e.

Datta S, Coussios CC, McAdory LE, Tan J, Porter T, Courten-Myers GD, Holland CK. Correlation of cavitation with ultrasound enhancement of thrombolysis. Ultrasound in Medicine & Biology, 2006;32:1257–1267.

de Jong N, Emmer M, Chin CT, Bouakaz A, Mastik F, Lohse D, Versluis M. "compression-only" behavior of phospholipid-coated contrast bubbles. Ultrasound in Medicine & Biology, 2007;33:653 – 656.

Fogler HS, Goddard JD. Collapse of spherical cavities in viscoelastic fluids. The Physics of Fluids, 1970;13:1135–1141.

Fransecutto A, Nabergoj R. "pulsation amplitude threshold for surface waves on oscillating bubbles". Acoustica, 1978;41:215–220.

Frinking PJA, de Jong N, Cspedes EI. Scattering properties of encapsulated gas bubbles at high ultrasound pressures. The Journal of the Acoustical Society of America, 1999;105:1989–1996.

Frizzell LA, Lee CS, Aschenbach PD, Borrelli MJ, Morimoto RS, Dunn F. Involvement of ultrasonically induced cavitation in the production of hind limb paralysis of the mouse neonate. The Journal of the Acoustical Society of America, 1983;74:1062–1065.

Frohly J, Labouret S, Bruneel C, Looten-Baquet I, Torguet R. Ultrasonic cavitation monitoring by acoustic noise power measurement. The Journal of the Acoustical Society of America, 2000;108:2012–2020.

Gasperoni C, Salgarello M. The use of external ultrasound combined with superficial subdermal liposuction. Annals of Plastic Surgery, 2000;45:369–373.

Goertz D, Hynynen K. Ultrasound-mediated drug delivery. Physics Today, 2016;69:30–36.

Guyton AC, Hall JE. Textbook of Medical Physiology, 11th Edition. Elsevier Saunders, Philadelphia, Pennsylvania, 2006. pp. 184–185.

Haar GT, Daniels S, Eastaugh KC, Hill CR. Ultrasonically induced cavitation in vivo. British Journal of Cancer. Supplement, 1982;5:151–155.

Hart J. The use of ultrasound therapy in wound healing. Journal of Wound Care, 1998;7:25–28.

Hauptmann M, Brems S, Struyf H, Mertens P, Heyns M, De Gendt S, Glorieux C. Time-resolved monitoring of cavitation activity in megasonic cleaning systems. Review of Scientific Instruments, 2012;83.

Hauptmann M, Struyf H, De Gendt S, Glorieux C, Brems S. Evaluation and interpretation of bubble size distributions in pulsed megasonic fields. Journal of Applied Physics, 2013;113.

Hockham N, Coussios CC, Arora M. A real-time controller for sustaining thermally relevant acoustic cavitation during ultrasound therapy. IEEE Transactions on Ultrasonics, Ferroelectrics, and Frequency Control, 2010;57:2685–2694.

Holland CK, Apfel RE. An improved theory for the prediction of microcavitation thresholds. IEEE Transactions on Ultrasonics, Ferroelectrics, and Frequency Control, 1989;36:204–208.

Holland CK, Deng CX, Apfel RE, Alderman JL, Fernandez LA, Taylor" KJ. "direct evidence of cavitation in vivo from diagnostic ultrasound". "Ultrasound in Medicine & Biology", 1996;22:917–925.

Holland CK, Roy RA, Apfel RE, Crum LA. In vitro detection of cavitation induced by a diagnostic ultrasound system. IEEE Transactions on Ultrasonics, Ferroelectrics, and Frequency Control, 1992;39:95–101.

Hsieh D, Plesset MS. Theory of rectified diffusion of mass into gas bubbles. The Journal of the Acoustical Society of America, 1961;33:206–215.

Keller MW, Glasheen W, Kaul S. Albunex: A safe and effective commercially produced agent for myocardial contrast echocardiography. Journal of the American Society of Echocardiography, 1989;2:48–52.

Kennedy JE, ter Haar GR, Cranston D. High intensity focused ultrasound: surgery of the future?

The British Journal of Radiology, 2003;76:590–599.

Klein J. Tumescent technique for regional anesthesia permits lidocaine doses of 35 mg/kg for liposuction. The Journal of dermatologic surgery and oncology, 1990;16:248–263.

Klein J. Tumescent technique for local-anesthesia improves safety in large-volume liposuction. Plastic and Reconstructive Surgery, 1993;92:1085–1098.

Klein J. ClinicalTrials.gov [Internet]. Bethesda (MD): National Library of Medicine (US). Identifier NCT02503904, Tumescent Antibiotic Delivery for Prevention of Surgical Site Infection, 2014. [cited 2017 Jun 26]; Available from: https://clinicaltrials.gov/ct2/show/NCT02503904.

Klein JA. Tumescent technique for lipo-suction surgery. The American Journal of Cosmetic Surgery, 1987;4:263–267.

Lauterborn W. Numerical investigation of nonlinear oscillations of gas bubbles in liquids. The Journal of the Acoustical Society of America, 1976;59:283–293.

Lauterborn W, Kurz T. Physics of bubble oscillations. Reports on Progress in Physics, 2010;73:106501.

Leighton TG. The Acoustic Bubble. Academic Press Limited, London, UK, Ch. 3, 1994.

Louisnard O, Gomez F. Growth by rectified diffusion of strongly acoustically forced gas bubbles in nearly saturated liquids. Phys. Rev. E, 2003;67:036610.

Marmottant P, van der Meer S, Emmer M, Versluis M, de Jong N, Hilgenfeldt S, Lohse D. A model for large amplitude oscillations of coated bubbles accounting for buckling and rupture. The Journal of the Acoustical Society of America, 2005;118:3499–3505.

Mendes FH. External ultrasound-assisted lipoplasty from our own experience. Aesthetic Plastic Surgery, 2000;24:270–274.

Minnaert M. Xvi. on musical air-bubbles and the sounds of running water. The London, Edinburgh, and Dublin Philosophical Magazine and Journal of Science, 1933;16:235–248.

Mitragotri S. Healing sound: the use of ultrasound in drug delivery and other therapeutic applications. Nature Reviews Drug Discovery, 2005;4:255–260.

Neppiras E, Coakley W. Acoustic cavitation in a focused field in water at 1 mhz. Journal of Sound and Vibration, 1976;45:341–373.

Nightingale KR, Church CC, Harris G, Wear KA, Bailey MR, Carson PL, Jiang H, Sandstrom KL, Szabo TL, Ziskin MC. Conditionally increased acoustic pressures in nonfetal diagnostic ultrasound examinations without contrast agents: A preliminary assessment. Journal of Ultrasound in Medicine, 2015;34:1–41.

Papadopoulou V, Eckersley RJ, Balestra C, Karapantsios TD, Tang MX. A critical review of physiological bubble formation in hyperbaric decompression. Advances in Colloid and Interface Science, 2013;191192:22–30.

Plesset MS, Prosperetti A. Bubble dynamics and cavitation. Annual Review of Fluid Mechanics, 1977;9:145–185.

Polat BE, Blankschtein D, Langer R. Low-frequency sonophoresis: application to the transdermal delivery of macromolecules and hydrophilic drugs. Expert Opinion on Drug Delivery, 2010;7:1415–1432.

Rapoport N. Phase-shift, stimuli-responsive perfluorocarbon nanodroplets for drug delivery to cancer. Wiley Interdisciplinary Reviews: Nanomedicine and Nanobiotechnology, 2012;4:492–510.

Rohrich RJ, Morales DE, Krueger JE, Ansari M, Ochoa O, Jr. JR, Beran SJ. Comparative lipoplasty analysis of in vivo-treated adipose tissue. Plastic & Reconstructive Surgery, 2000;105:2152–2158.

Rosenberg GJ, Cabrera RC. External ultrasonic lipoplasty: an effective method of fat removal and skin shrinkage. Plastic & Reconstructive Surgery, 2000;105:785–791.

Silberg BN. The technique of external ultrasound-assisted lipoplasty. Plastic and Reconstructive Surgery, 1998;101:552–553.

Silberg BN. Direct antibiotic delivery into soft tissue infections using ultrasonic dispersion. Supplement to Plastic and Reconstructive Surgery, 2013;132:51–52.

ter Haar G, Daniels S, Eastaugh KC, Hill CR. Ultrasonically induced cavitation in vivo. Br J Cancer Suppl., 1982;5:151–155.

Tikuisis P. Modeling the observations of in vivo bubble formation with hydrophobic crevices. Undersea Biomedical Research, 1986;13:165–180.

Tomizawa M, Shinozaki F, Motoyoshi Y, Sugiyama T, Yamamoto S, Sueishi M. Sonoporation: gene transfer using ultrasound. World Journal of

Methodology, 2013;3:39–44.
Weninger K, Camara C, Putterman S. Physical acoustics of ultrasound-assisted lipoplasty. Clinics in Plastic Surgery, 1999;26:463–79.
Weninger KR, Camara CG, Putterman SJ. Observation of bubble dynamics within luminescent cavitation clouds: Sonoluminescence at the nano-scale. Phys. Rev. E, 2000;63:016310.
Xu Z, Ludomirsky A, Eun LY, Hall TL, Tran BC, Fowlkes JB, Cain CA. Controlled ultrasound tissue erosion, 2004;51:726–736.
Yang X, Church CC. A model for the dynamics of gas bubbles in soft tissue. J. Acoust. Soc. Am., 2005;118:3595–3606.
Zocchi M. Ultrasonic liposculpturing. Aesthetic Plastic Surgery, 1992;16:287–298.